OCTOBER 1975 MATT-1163

RESISTIVE INSTABILITIES IN A TOKAMAK

BY

A. H. GLASSER, J. M. GREENE,
AND
J. L. JOHNSON

PLASMA PHYSICS LABORATORY

PRINCETON UNIVERSITY
PRINCETON, NEW JERSEY

This work was supported by U. S. Energy Research and Development Administration Contract E(11-1)-3073. Reproduction, translation, publication, use and disposal, in whole or in part, by or for the United States Government is permitted.

DISCLAIMER

NOTICE

Printed in the United States of America.

Available from
National Technical Information Service
U. S. Department of Commerce
5285 Port Royal Road
Springfield, Virginia 22151
Price: Printed Copy $ *; Microfiche $1.45

*Pages	NTIS Selling Price
1-50	$ 4.00
51-150	5.45
151-325	7.60
326-500	10.60
501-1000	13.60

RESISTIVE INSTABILITIES IN A TOKAMAK

A. H. Glasser, J. M. Greene, and J. L. Johnson*

Plasma Physics Laboratory, Princeton University

Princeton, New Jersey 08540

ABSTRACT

Application of resistive instability theory shows that toroidal effects can stabilize the tearing mode in devices like the Princeton Large Torus. Contraction of the current channel is destabilizing. Finite fluid compressibility is crucial to this phenomenon.

1. INTRODUCTION

The Mirnov oscillations frequently observed in tokamak discharges[1,2] are generally interpreted as resistive instabilities, specifically tearing modes, driven unstable by the Ohmic heating current.[3,4,5] The analysis is usually done for a straight, cylindrical model tokamak. The effects of toroidal curvature are neglected on the ground that the singular layer where resistivity is important is unaffected by curvature because it is so narrow.[5] Glasser, et al[6] have treated resistive instabilities in an arbitrarily shaped toroidal plasma. Curvature effects enter the analysis because the perturbations, which are constant along a field line on the singular surface, sample varying equilibrium quantities such as the toroidal and poloidal magnetic field strengths. Although these effects are small in a tokamak, they have a strong influence on the stability of the resistive modes because the resistivity is so small.

In this paper we apply the theory of Ref. 6 to a tokamak with large aspect ratio, circular cross section, and arbitrary current and pressure profiles. We find that toroidal effects are sufficient to stabilize the tearing mode in devices such as the ST tokamak if the current profile is rather flat, but contraction of the current channel destabilizes it. The PLT device should be much more stable because of its smaller aspect ratio and higher temperature.

In Sec. II we describe the equilibrium. In Sec. III we discuss the stability properties of the system and give numerical

results for the ST and PLT tokamaks. We also show that allowance for finite fluid compressibility is crucial for deriving toroidal stabilization. In Sec. IV we summarize our results. In the Appendix we evaluate the critical parameters of Ref. 6 which are needed in Sec. III.

II. EQUILIBRIUM

We treat an axisymmetric toroidal equilibrium, with the magnetic field given by

$$\vec{B} = \frac{1}{2\pi} \vec{\nabla}\phi \times \vec{\nabla}\chi + RB_o g(\chi)\vec{\nabla}\phi \ , \qquad (1)$$

where ϕ is the angle about the axis of symmetry, χ is the poloidal flux, R is the distance from the axis of symmetry to the magnetic axis, and B_o is the externally imposed toroidal magnetic field strength at the magnetic axis. As in the earlier work,[6] we use rationalized electromagnetic units. To convert to Gaussian CGS units,[7] make the substitutions

$$\vec{B}\to\vec{B}/\sqrt{4\pi} \ , \quad \vec{J}\to\sqrt{4\pi}\ \vec{J}/c \ , \ \eta\to\eta c^2/4\pi \quad ; \qquad (2)$$

for rationalized MKS units, use

$$\vec{B}\to\vec{B}/\sqrt{\mu_o} \ , \quad \vec{J}\to\sqrt{\mu_o}\ \vec{J} \ , \ \eta\to\eta/\mu_o \quad . \qquad (3)$$

A combination of Ampere's law and pressure balance gives the well-known equilibrium equation,

$$X^2\vec{\nabla}\cdot\left(\frac{1}{X^2}\vec{\nabla}\chi\right) = 2\pi XJ\hat{\phi} = -4\pi^2(R^2R_o^2gg' + X^2p') \ , \qquad (4)$$

with X the radius from the axis of symmetry, $p(\chi)$ the pressure, J_ϕ the toroidal current density, and primes denoting derivatives with respect to χ .

We consider large-aspect- ratio solutions of Eq. (2), writing

$$X = R + r\cos\theta, \quad z = r\sin\theta, \quad r/R \sim \varepsilon << 1 , \tag{5}$$

where z is the distance along the axis of symmetry, r and θ are circular coordinates about the magnetic axis at X = R, z = 0, and ε is the inverse aspect ratio. We seek series solutions of the form

$$\begin{aligned} \chi(r,\theta) &= \chi^{(o)}(r) + \varepsilon\chi^{(1)}(r,\theta) + \ldots , \\ g(\chi) &= 1 + \varepsilon^2 g^{(2)}(r) + \varepsilon^3 g^{(3)}(r,\theta) + \ldots , \\ p(\chi) &= \varepsilon^2 p^{(2)}(r) + \varepsilon^3 p^{(3)}(r,\theta) + \ldots , \end{aligned} \tag{6}$$

which are circularly symmetric in lowest order. If we prescribe the pressure $p(\chi)$ and the safety factor

$$\begin{aligned} q(\chi) &\equiv \frac{RB_o g}{2\pi}\oint \frac{d\theta}{X^2 \vec{B}\cdot\vec{\nabla}\theta} \\ &= q^{(o)}(r) + \varepsilon q^{(1)}(r,\theta) + \ldots , \end{aligned} \tag{7}$$

where the integral is taken around a poloidal cross section at constant χ, or equivantly prescribe $p^{(2)}(r)$ and $q^{(o)}(r)$, then the first terms in the solution are[8]

$$\chi^{(o)}(r) = 2\pi B_o \int_o^r \frac{r'\,dr'}{q^{(o)}(r')} , \tag{8}$$

$$\chi^{(1)}(r) = \cos\theta \frac{2\pi B_o r}{R q^{(o)}} \int_o^r dr' \frac{q^{(o)2}}{r'^3} \int_o^{r'} dr'' \left(\frac{r''^3}{q^{(o)2}} - 2 \frac{R^2 r''^2}{B_o^2} \frac{dp^{(2)}}{dr'} \right), \quad (9)$$

$$J_\phi^{(o)}(r) = \frac{B_o}{Rr} \frac{d}{dr} \frac{r^2}{q^{(o)}(r)}, \quad (10)$$

$$g^{(2)}(r) = \frac{1}{R^2} \int_r^a \frac{dr'}{q^{(o)}} \frac{d}{dr'} \frac{r'^2}{q^{(o)}} - \frac{p^{(2)}(r)}{B_o^2}. \quad (11)$$

III. STABILITY

The stability of the system is determined by a set of parameters defined in Eq. (13) of Ref. 6. These are evaluated in the Appendix of this work for the equilibrium of Sec. II. In this section we examine the conditions for stability against the various modes treated in Ref. 6 and summarized in Sec. VI of that paper. We first show that the ideal magnetohydrodynamic interchange is very effectively stabilized by shear. We then consider conditions for the stability of the resistive interchange. Using a particular model of the current and pressure profiles and the numerical results of Furth et al,[5] we then show that the same favorable curvature which stabilizes the resistive interchange can stabilize the tearing mode in the ST and PLT tokamaks. The result is first obtained by treating the parameters G and H as small. Then, in discussing the effects of large G, we show that allowance for finite fluid compressibility is necessary to obtain curvature stabilization. Finally, we show that the effects of H will be significant in PLT.

A. Interchange Modes

The rapidly-growing ideal magnetohydrodynamic interchange is unstable unless the Mercier criterion,

$$D_I \equiv E + F + H - 1/4$$
$$= \frac{2q^{(o)2}}{B_o^2 r} \frac{dp^{(2)}}{dr} \left(\frac{q^{(o)}}{dq^{(o)}/dr}\right)^2 \left(1 - \frac{1}{q^{(o)2}}\right) - \frac{1}{4} \qquad (12)$$
$$< 0 ,$$

is satisfied. It is interesting to note that the terms F and H, Eqs. (A19) and (A21), cancel all but the first two terms of E, Eq. (A18). Since these terms are of order ε^2 they are generally much smaller than the term -1/4, which represents shear stabilization, and thus the Mercier criterion is nearly always satisfied. Although it can be violated, for example if $dp^{(2)}/dr<0$, $q^{(o)}<1$, and $dq^{(o)}/dr$ vanishes, this would be exceptional. It can occur in the immediate vicinity of the magnetic axis.

The resistive interchange is unstable unless[9]

$$D_R \equiv E + F + H^2$$
$$= \frac{2q^{(o)2}}{B_o^2 r} \frac{dp^{(2)}}{dr} \left(\frac{q^{(o)}}{dq^{(o)}/dr}\right)^2 \left[1 - \frac{1}{q^{(o)2}}\right.$$
$$\left. + \frac{q^{(o)}}{r^3} \frac{dq^{(2)}}{dr} \int_o^r dr' \left(\frac{r'^3}{q^{(o)2}} - \frac{2R^2 r'^2}{B_o^2} \frac{dp^{(2)}}{dr'}\right)\right] \qquad (13)$$
$$< 0 .$$

This is always more stringent than the Mercier criterion, since

$$D_R - D_I = (H - 1/2)^2 > 0 \ . \qquad (14)$$

The term H^2, while destabilizing, is of order ε^4 and therefore negligible compared to the other terms of D_R, which are of order ε^2 The shear stabilization term - 1/4 of D_I does not occur in D_R . The integral terms in Eq.(13) are the terms of E which are cancelled by H in D_I . If $dp^{(2)}/dr < 0$ and $dq^{(o)2}/dr > 0$ everywhere, they are stabilizing. If, in addition, $q^{(o)}>1$, $D_R < 0$ everywhere and the resistive interchange is stable. As discussed in Sec. VI of Ref. 6 , average toroidal field-line curvature then provides stabilization by decreasing D_R.

B. Tearing Modes with G and H Small

If $D_R<0$, we must consider the stability of the tearing mode. This depends on the parameter Δ, defined in Eq.(84) of Ref. 6, which arises in matching the solutions inside the resistive layer to the solutions in the ideal regions on either side of it. For H = 0 it is the jump in the logarithmic derivative of the normal component of the perturbed magnetic field across the singular layer. It carries the destabilizing influence of the Ohmic heating current. For the equilibrium treated here, and for poloidal mode numbers m > 1, it is given correctly to lowest order by the cylindrical approximation, and is unaffected by the pressure profile. It is evaluated for several profiles $q^{(o)}(r)$ in Ref. 5. If $D_R = 0$, the tearing mode is unstable for $\Delta > 0$, as discussed in Ref. 5. But if $D_R < 0$, the mode is converted to the modified tearing mode

with a complex frequency, and is unstable only if $\Delta > \Delta_C$, where

$$\Delta_C \approx 1.54\ (V_S/X_o)|D_R|^{5/6} \qquad (15)$$

when G and H are small. The large factor V_S/X_o is the ratio of a macroscopic scale length to the resistive layer thickness. It is given by Eq.(A31). Because of this large factor, curvature stabilization can be important even though D_R is small.

To determine the magnitudes of D_R and Δ_C and compare them to the values of Δ, we use the peaked model of Ref. 5, in which $q^{(o)}$ is a quadratic function of r. We also use a parabolic pressure profile. These profiles are given by

$$p^{(2)}(r) = p_o(1-r^2/a^2) , \qquad (16)$$

$$q^{(o)}(r) = q_o(1+sr^2/a^2) , \qquad (17)$$

where a is the limiter radius. We call the constant s a shear parameter, since $dq^{(o)}/dr = 2q_o sr/a^2$. The radial variable used in Ref. 5 is $x \equiv r/r_o$, with $r_o \equiv a/\sqrt{s}$. The current density is given by

$$J_\phi^{(o)} = J_o/(1+sr^2/a^2) , \qquad (18)$$

$$J_o = 2B_o/q_oR = (1+s)I/\pi a^2 , \qquad (19)$$

where I is the total toroidal current. As s increases, the current channel contracts, as it normally does during the course of a tokamak discharge due to the thermal instability of the Ohmic heating current.[10] If I is held fixed during this contraction, q_o falls, while if q_o is held fixed, I falls. It is convenient to

express p_o in terms of

$$\beta_p \equiv \left[\frac{2Rq^{(o)}(a)}{B_o a^2}\right]^2 \int_o^a dr\ r\ p(r) \quad ; \tag{20}$$

$$p_o = \frac{\beta p}{(1+s)^2} \left(\frac{B_o a}{q_o R}\right)^2 \quad . \tag{21}$$

Note that β_p is of order unity in the aspect ratio expansion.

With these profiles, we obtain

$$D_R = -\frac{\beta_p a^4}{s^2 R^2 r^2} \frac{(1+sr^2/a^2)^4}{(1+s)^2} \left[\left(\frac{1+sr^2/a^2}{sr^2/a^2}\right) \ln(1+sr^2/a^2) - \frac{1}{q_o^2 (1+sr^2/a^2)^2} + \frac{2\beta_p}{(1+s)^2} \frac{sr^2}{a^2} (1+sr^2/a^2)\right] . \tag{22}$$

If $q_o > 1$, $D_R < 0$ everywhere, and is therefore stabilizing. If $q_o < 1$, $D_R > 0$ in the vicinity of the axis, and the resistive interchange is unstable. If this occurs, the resultant instability will flatten the profiles and return q_o to one or greater. We therefore consider the case for which q_o is held fixed at 1.1. The solid curves in Fig. 1 show values of $|D_R|$ vs. r/a between the axis and the limiter for values of s between 1 and 3, with $\beta_p = 0.8$ and $R/a = 8.4$, appropriate for the ST tokamak. The behavior at the axis is sensitive to the particular model employed. If q_o were less than 1, they would diverge with the opposite sign. If $p^{(2)}$ were flatter at the axis, they would remain finite. The open circles denote the q = 2 surfaces, while the solid circles denote the q = 3 surfaces. As s increases and the current channel shrinks, $|D_R|$ decreases, and its stabilizing influence is lost. Since the integral q surfaces also move in and down the curves as s increases, each mode is destabilized even faster. The dashed

curve is for R/a = 2.9, appropriate for PLT, with s = 2. The values of $|D_R|$ for a given value of s are due to the smaller aspect ratio. The shrinking of the current channel can be thought of as an increase of the effective aspect ratio, leading to a reduction of the curvature effects.

Figure 2 is a graph of $r_o\Delta_c$ as a function of r/a . The general features are similar to those in Fig. 1, but the variations are even more pronounced because of the effects of varying resistivity. We use the Spitzer resistivity[11] enhanced by a factor Z_{eff}, chosen as 2.5 for ST and 1.5 for PLT, to account for impurities. We take the electron temperature in ST to be 2.5 keV, while for PLT we use 4.0 keV. We take the radial dependence of η to be inversely proportional to $J_\phi^{(o)}(r)$. The s = 2 curve for PLT is off scale here because of its higher temperature, so we show the s = 3 curve. The curves drop more steeply with increasing s because of the radial increase of η. The horizontal line near the bottom is the value of $r_o\Delta$ calculated in Ref. 5 for the m = 2, n = 1 mode. While the analysis of that reference predicts instability for the mode because Δ is positive, we find it to be stable until s reaches about 2.5 and Δ_c drops below Δ at the q = 2 surface. For the m = 3 mode, this model gives a negative value of Δ for these parameters, so it is stable. Increasing q_o would raise Δ, and eventually give the m = 3 mode a positive value of Δ, in general less than that associated with m = 2.

The higher values of Δ_c for PLT indicate that the m = 2 mode is much more stable than in ST. This is also seen in Fig. 3,

which shows $r_o \Delta_c$ vs. s at the q = 2 surface in ST and PLT. While ST goes unstable to the m = 2 mode when s reaches 2.4, PLT remains stable until s reaches 7.5 . Since the contraction of the current channel is caused by the thermal instability of the Ohmic heating current, and since PLT will derive much of its heat from neutral injection, s may never reach this value.

The growth or damping rate for the m = 2 mode is of order $5 \times 10^3 sec^{-1}$ in ST and slightly lower in PLT. This is comparable to the growth rates of the observed m = 2 Mirnov oscillations,[1,2] but much smaller than the electron diamagnetic rotation frequency $\omega_e^* \approx 10^5 sec^{-1}$ which has not been included in our treatment.[12-15] Since it is also comparable to the electron collision frequency $\nu_e \approx 2 \times 10^4 sec^{-1}$, this should be incorporated in the theory.[12,15] Similarly, the resistive layer thickness δr, Eq. (A32), is of order $3 \times 10^{-2} cm.$, and thus smaller than the ion gyration radius, which is of order $8 \times 10^{-2} cm.$ This indicates that the treatment should include the effects of finite ion gyration radius.[13,16] These effects will be considered in future papers.

C. The Effects of G and H

The expression for Δ_c given in Eq. (15) is valid only if G and H are small. It can be seen from Eq. (A20) that G is not small but large, of order ε^{-2}; in fact, $G = 2/\gamma\beta$, and $\beta \lesssim 10^{-2}$ in a tokamak. However, it can be seen in Fig. 4 that G has a very weak effect on Δ_c . There are two reasons for this. First, the Appendix of Ref. 6 shows that G enters the dispersion relation only through the combination GD_R when $Q^{3/2}$ is scaled to D_R. Since D_R is proportional to ε^2 and β, this product is of order unity

and independent of β. A graph of $|GD_R|$ vs. r/a for ST and PLT with s = 2, shown in Fig. 5, indicates that the product is still rather large.

The second reason why G is not very important is the weak dependence of Δ_C on GD_R, as shown in Fig. 4. For $|GD_R| << 1$, $\Delta_C = \Delta_o$, the value given in Eq. (15), while for $GD_R >> 1$,

$$\Delta_C \approx 1.303 \, |GD_R|^{-1/6} \, \Delta_o \, . \tag{23}$$

This scaling with GD_R can also be obtained analytically by introducing a small parameter $\delta << 1$ and the ordering

$$GD_R \sim G^2 Q^3 \sim D_R^2/Q^3 \sim \delta^{-1} \tag{24}$$

into Eqs. (A5), (A9), and (A10) of Ref. 6. Stirling's formula is used to determine the ratio of gamma functions in Eq. (A9) as $(-R_\pm/4)^{-1/4}$, with $|\arg(-R_\pm)| < \pi$. The resulting expression for $\Delta'(Q)$ is a product of $|D_R|^{5/6}/|GD_R|^{1/6}$ times a complex function of the variable GQ^3/D_R. Since we are interested in marginal stability, we take Re Q= 0. The imaginary part of $\Delta'(Q)$ vanishes for

$$Q = 0.628 \, i|D_R/G|^{1/3} \, , \tag{25}$$

while the real part yields Eq. (23). Figure 6 shows Δ_C/Δ_o vs. r/a for ST and PLT with s = 2. The value of Δ_C is reduced by 24 percent at the q = 2 surface. For larger values of s, the approximation $\Delta_C \approx \Delta_o$ is even better. Only near the axis and the limiter does the approximation get bad.

It is stated in the Appendix of Ref. 5 that the effects of toroidal curvature cannot stabilize the tearing mode. This conclusion is based on a low-pressure approximation, given in Eq. (109) of Ref. 4, in which

$$G \sim \delta^{-2}, \quad D_R \sim Q^{3/2} \sim \delta . \tag{26}$$

This is equivalent to the limit $|GD_R| \to \infty, \Delta_C \to 0$ in Fig. 4, and thus misses the stabilizing effect of D_R through Δ_C. It can be seen in Fig. 6 that this limit is not appropriate to a tokamak.

There are two approximations frequently made in treating resistive instabilities that lead to this same misleading conclusion. If the ordering of Eq. (26) is introduced into Eq. (23) of Ref. 6, the lowest-order terms in the equation give $\Xi = T$. If this approximation is introduced into Eqs. (9) and (22), the constant-Ψ approximation leads to the dispersion relation appropriate to the limit $|GD_R| \to \infty$. The approximation $\Xi = T$ also follows from the assumption that the fluid motion is incompressible, so the $\vec{\nabla} \cdot \vec{\xi} = 0$, instead of adiabatic, with $\vec{\nabla} \cdot \vec{\xi} \sim \varepsilon$, as in Ref. 6. This can be seen by taking the scaler product of Eq. (4) in Ref. 6 with $\vec{\nabla} V \times \vec{\nabla} \theta$ and using the ordering in Eq. (6) of that work. The use of a fictitious gravitational field to simulate the effects of curvature in a slab model, as in Ref. 3, also leads to this inappropriate limit, since the mass density perturbation which would then enter Eq. (4) of Ref. 6 would lead to a term proportional to Ξ rather than T in Eq. (22) of Ref. 6.

While the parameter H, Eq. (A21), is of order ϵ^2, it can have a significant effect on Δ_C. Figure 9 shows the behavior of the dimensionless ratio $r_o^{-2H}\Delta_C/\Delta_o$ as a function of H, where Δ_C is given by Eq. (111) of Ref. 6 and Δ_o is the value of Δ_C for H = 0, given by Eq. (15), with D_R held fixed at -0.01 and $r_o V_s/X_o$ held fixed at 250.[17] This shows that Δ_C is reduced by a factor of 2 for H ≈ 0.1 . For the peaked model, Eqs. (16) and (17), H is given by

$$H = \frac{\beta_p a^4}{s^2 R^2 r^2} \frac{(1 + sr^2/a^2)^4}{(1 + s)^2} \left[\left(\frac{1 + sr^2/a^2}{sr^2/a^2} \right) \ln(1 + sr^2/a^2) - 1 \right.$$

$$\left. + \frac{2\beta_p}{(1 + s)^2} \frac{sr^2}{a^2} \left(1 + \frac{sr^2}{a^2}\right) \right] \qquad (27)$$

Figure 8 shows the value of H in the ST and PLT tokamaks as a function of minor radius with s = 2. Figure 9 shows the corresponding variation of $r_o^{-2H}\ \Delta_C/\Delta_o$ as a function of minor radius. While the effect of H is very small in ST, it should be significant in PLT. As s increases, H decreases, and its effect is reduced.

There are two further difficulties in determining the influence of H on the stability of the system. First, while the treatment in the main body of Ref. 6 gives the effects of H when G is small, and the treatment in the Appendix of that work gives the effects of G when H is small, neither treatment gives the combined effects of G and H. Figures 6 and 9 indicate that this could be important in PLT. These effects must be determined by a numerical solution of Eqs. (9) through (12) of Ref. 6, and will be treated in a future paper.

The second difficulty is that the cylindrical approximation used in Ref. 5 to determine Δ from the solution of the ideal equations in the outer regions may not be valid when H is large enough to affect Δ_c. The definition of H in Eq. (A21) shows the H vanishes in a cylinder. The asymptotic behavior of the inner solutions, given in Eq. (82) of Ref. 6, shows that for $H \neq 0$, the power-like terms do not match those in a cylinder, and this affects the definition of Δ. Thus, we do not know the behavior of Δ for $H \neq 0$, and we cannot predict the stability boundary. This behavior could be determined from a two-dimensional numerical computation in the outer region,[18] and will be treated in a later work.

IV. DISCUSSION

To summarize our results, we have shown how to apply the resistive stability theory of Ref. 6 to a large-aspect-ratio tokamak with a circular cross section and arbitrary current and pressure profiles. We have given numerical results appropriate to the ST and PLT tokamaks. These results indicate that toroidal curvature can stabilize the tearing mode in the ST tokamak if the current profile is sufficiently flat, but that contraction of the current channel destabilizes it. The PLT tokamak is expected to be more stable because of its smaller aspect ratio and higher temperature. We have shown that the parameters G and H of Ref. 6 have a small effect on stability, and that finite fluid compressibility is crucial. These results are used to show why the stabilization found here was not seen previously.

For $q_o < 1$, the internal kink mode, an m = 1 ideal magnetohydrodynamic instability which has recently received considerable attention,[19,20] is expected to be unstable. A recent treatment of this mode shows that the value of Δ obtained in the outer region where the ideal equations apply is strongly affected by toroidal curvature, and cannot be treated in the cylindrical approximation.[21] A second reason sometimes given for the special nature of this mode is that the value of the perturbed magnetic field at the singular surface vanishes, invalidating the constant-ψ approximation and leading to an infinite value of Δ. This is strictly true only in the cylindrical approximation; toroidal corrections show that $\Delta \sim R/a$, which is not too large to be included in the theory of Ref. 6. More effort is needed to determine the relation between this mode and the modes treated here and in Ref. 6.

Despite the need for further generalization of the model that has been pointed out, these results indicate that magnetohydrodynamic instabilities should pose less severe limitations on PLT than on ST.

ACKNOWLEDGMENTS

We appreciate P. H. Rutherford's interest in and encouragement of this work. We gratefully acknowledge useful discussions with J. Finn and S. von Goeler.

This work was supported by the U. S. Energy Research and Development Administration Contract E(11-1)-3073. Use was made of computer facilities supported in part by National Science Foundation Grant NSF-GP 579.

APPENDIX

In this Appendix we evaluate the equilibrium quantities E, F, G, H, K, and M, and the scale factors Q_o, X_o, and V_s, defined in Eqs. (13), (14), and (81) of Ref. 6. We give details of the calculation of E, and only the results for the others.

For axisymmetric field in Eq. (1), E is given by

$$E \equiv \frac{p'V'}{q'^2} \left\langle \frac{B^2}{|\vec{\nabla}\chi|^2} \right\rangle \left[(2\pi RB_o gq'/\langle B^2 \rangle) - V'' \right] , \tag{A1}$$

where

$$V(\chi) \equiv \int d\tau \tag{A2}$$

is the volume contained within a surface of constant χ ,

$$V' = \oint d\theta / \vec{B}\cdot\vec{\nabla}\theta \tag{A3}$$

and the field-line average of any quantity A is

$$\langle A \rangle \equiv \frac{1}{V'} \oint \frac{d\theta}{\vec{B}\cdot\vec{\nabla}\theta} A \quad , \tag{A4}$$

with the integrals taken around a poloidal cross section at constant χ. We also use the relations

$$\Phi(\chi) = \frac{RB_o}{2\pi} \oint d\tau \frac{g}{X^2} \quad , \tag{A5}$$

$$q = \Phi' \quad , \tag{A6}$$

$$\Lambda = -q'/V'^3 \quad , \tag{A7}$$

$$J' = -2\pi RB_o g' \quad , \tag{A8}$$

$$\sigma = -2\pi RB_o (g' + gp'/B^2) \quad . \tag{A9}$$

The toroidal flux Φ was denoted by ψ in Ref. 6.

The lowest-order terms inside the brackets of Eq. (A1) exactly cancel. To find the first nonvanishing contributions, it is necessary to determine V, Φ, and $\langle B^2 \rangle$ to higher order. The volume V is

$$V(\chi) = 2\pi \int_0^{2\pi} d\theta \int_0^{r(\chi,\theta)} dr\, rX - \pi R \int_0^{2\pi} d\theta\, r^2(\chi,\theta)\left[1 + \frac{2}{3R} r(\chi,\theta)\cos\theta\right] \quad (A10)$$

We invert the power series solution for $\chi(r,\theta)$ of Eq. (4), Eqs. (8) and (9), to determine $r(\chi,\theta)$ iteratively as

$$r(\chi,\theta) = r^{(o)}(\chi) + r^{(1)}(\chi)\cos\theta + r_o^{(2)}(\chi) + r_2^{(2)}\cos 2\theta + \ldots , \quad (A11)$$

$$r^{(o)}(\chi) = \chi^{(o)-1}(\chi) , \quad (A12)$$

$$r^{(1)}(\chi) = -\left.\frac{\chi^{(1)}}{d\chi^{(o)}/dr}\right|_{r^{(o)}} . \quad (A13)$$

While $r_o^{(2)}$ and $r_2^{(2)}$ involve the second-order solution $\chi^{(2)}(r,\theta)$, these terms cancel out of E and the first-order solution is sufficient. Then

$$V(\chi) = 2\pi^2 R r^{(o)2}\left[1 + \frac{1}{2}\left(\frac{r^{(1)}}{r^{(o)}}\right)^2 + 2\frac{r_o^{(2)}}{r^{(o)}} + \frac{r^{(1)}}{R}\right] + \ldots . \quad (A14)$$

Similarly,

$$\Phi(\chi) = B_o \int_0^{2\pi} d\theta \int_0^{r(\chi,\theta)} dr\, r\, g/X$$

$$= \pi B_o r^{(o)2}\left[1 + \frac{1}{2}\left(\frac{r^{(1)}}{r^{(o)}}\right)^2 + 2\frac{r_o^{(2)}}{r^{(o)}} - \frac{r^{(1)}}{R} + \frac{1}{4}\left(\frac{r^{(o)}}{R}\right)^2 + \frac{2}{r^{(o)2}}\int_0^{r^{(o)}} dr\, r\, g^{(2)}(r)\right] + \ldots , \quad (A15)$$

so that

$$\frac{V'}{\Phi'} = \frac{2\pi R}{B_o}\left[1 - \frac{1}{r}\frac{d}{dr}\left(\frac{r^2\chi^{(1)}}{R d\chi^{(o)}/dr}\right) - \frac{1}{2}\frac{r^2}{R^2} - g^{(2)}\right] + \cdots \quad (A16)$$

Using $R B_o g\langle 1/X^2\rangle = 2\pi\Phi'/V'$ in the expression for $\langle B^2\rangle$, we find

$$\frac{2\pi R B_o g\Phi'}{\langle B^2\rangle} - V'' = \frac{V'\Phi''}{\Phi'}\left[1 - \frac{V'}{2\pi R B_o g\Phi'}\left\langle\frac{|\vec{\nabla}\chi|^2}{(2\pi X)^2}\right\rangle\right] - V'' + \cdots$$

$$= -\Phi'\left(\frac{V'}{\Phi'}\right) - \left(\frac{V'}{\Phi'}\right)^2\left\langle\frac{|\vec{\nabla}\chi|^2}{(2\pi X)^2}\right\rangle\left(\frac{\Phi''}{2\pi R B_o g\Phi'}\right) + \cdots$$

$$= \frac{q^{(o)2}}{RB_o^2}\left\{\frac{R}{r^3}\frac{d}{dr}\left[r^3\frac{d}{dr}\left(\frac{\chi^{(1)}}{d\chi^{(o)}/dr}\right)\right] + 1\right.$$

$$\left. + \frac{R^2}{r}\left[\frac{dg^{(2)}}{dr} - \frac{r}{q^{(o)3}}\frac{dq^{(o)}}{dr}\right]\right\} + \cdots \quad . \quad (A17)$$

Then, using Eqs. (8), (9), and (11), we obtain

$$E = \frac{2q^{(o)2}}{B_o^2 r}\frac{dp^{(2)}}{dr}\left(\frac{q^{(o)}}{dq^{(o)}/dr}\right)^2\left[1 - \frac{1}{q^{(o)2}}\right.$$

$$+ \frac{q^{(o)}}{r^3}\frac{dq^{(o)}}{dr}\int_o^r dr'\left(\frac{r'^3}{q^{(o)2}} - 2\frac{R^2 r'^2}{B_o^2}\frac{dp^{(2)}}{dr'}\right)$$

$$\left. - \frac{R^2 q^{(o)2}}{B_o^2 r}\frac{dp^{(2)}}{dr}\left(1 + \frac{1}{2q^{(o)2}}\right)\right] + \cdots \quad . \quad (A18)$$

Of the remaining parameters, F and H require expansion to second order, as with E, while G, K, and M can be evaluated with the

lowest-order fields. The results are:

$$F \equiv \left(\frac{p'V'}{q'}\right)^2 \left[(2\pi RB_o g)^2 \left(\left\langle\frac{B^2}{|\nabla\chi|^2}\right\rangle \left\langle\frac{1}{B^2|\nabla\chi|^2}\right\rangle - \left\langle\frac{1}{|\nabla\chi|^2}\right\rangle^2\right) + \left\langle\frac{B^2}{|\nabla\chi|^2}\right\rangle \left\langle\frac{1}{B^2}\right\rangle\right]$$

$$= \frac{2q^{(o)2}}{B_o{}^2 r} \frac{dp^{(2)}}{dr} \left(\frac{q^{(o)}}{dq^{(o)}/dr}\right)^2 \left[\frac{R^2 q^{(o)2}}{B_o{}^2 r} \frac{dp^{(2)}}{dr}\left(1 + \frac{1}{2q^{(o)2}}\right)\right] + \ldots , \tag{A19}$$

$$G \equiv \langle B^2\rangle / M\gamma p = B_o{}^2/\gamma p^{(2)} + \ldots , \tag{A20}$$

where $\gamma = 5/3$ in the ratio of specific heats,

$$H \equiv (2\pi RB_o g p'V'/q') \left(\left\langle\frac{1}{|\vec{\nabla}\chi|^2}\right\rangle - \frac{\langle B^2/|\vec{\nabla}\chi|^2\rangle}{\langle B^2\rangle}\right) \tag{A21}$$

$$= -\frac{2q^{(o)2}}{B_o{}^2 r} \frac{dp^{(2)}}{dr} \left(\frac{q^{(o)}}{dq^{(o)}/dr}\right)^2$$

$$\times \left[-\frac{q^{(o)}}{r^3} \frac{dq^{(o)}}{dr} \int_o^r dr' \left(\frac{r'^3}{q^{(o)2}} - 2\frac{R^2 r'^2}{B_o{}^2} \frac{dp^{(2)}}{dr}\right)\right] + \ldots ,$$

$$K = \left(\frac{q'}{p'V'}\right)^2 \frac{\langle B^2\rangle}{M\langle B^2/|\vec{\nabla}\chi|^2\rangle}$$

$$= \left(\frac{B_o{}^2 r}{Rq^{(o)2}} \frac{dq^{(o)}/dr}{dp^{(2)}/dr}\right)^2 \tag{A22}$$

$$M \equiv \left\langle\frac{B^2}{|\vec{\nabla}\chi|^2}\right\rangle \left[\left\langle\frac{|\nabla\chi|^2}{B^2}\right\rangle + (2\pi RB_o g)^2 \left(\left\langle\frac{1}{B^2}\right\rangle - \frac{1}{\langle B^2\rangle}\right)\right] = 1 + \ldots . \tag{A23}$$

Note that E, F, and H are of order ε^2, while G and K are of order ε^{-2}.

A number of scale factors are defined in Ref. 6, and they must also be evaluated. Perturbations vary as exp [i(mθ-nφ-ωt)], where m and n are integers satisfying m = nq(χ_o), with χ_o the singular surface. The complex frequency ω (denoted by q in Ref. 6) is given by

$$\omega = iQQ_o \quad . \tag{A24}$$

Here, Q is a dimensionless, complex quantity, determined by solving a dispersion relation. The scale factor Q_o is given by

$$Q_o \equiv \left(\frac{\eta \alpha^2 \Lambda^2 \langle B^2 \rangle}{\rho M \langle B^2 / |\vec{\nabla} V|^2 \rangle} \right)^{1/3}$$

$$= \left[\frac{\eta}{\rho} \left(\frac{nB_o}{Rq^{(o)}} \frac{dq^{(o)}}{dr} \right)^2 \right]^{1/3} \quad , \tag{A25}$$

with $\alpha = 2\pi n V' = 2\pi m V'/\Phi'$, η the resistivity, and ρ the mass density, all evaluated on the singular surface.

The microscopic, dimensionless variable X describing the distance from the singular surface is given by

$$X \equiv (V - V_o)/X_o \quad , \tag{A26}$$

with the scale factor X_o given by

$$X_o \equiv \left(\frac{\rho M \eta^2 \langle B^2 \rangle^2}{\alpha^2 \Lambda^2 \langle B^2 / |\vec{\nabla} V|^2 \rangle} \right)^{1/3}$$

$$= 4\pi^2 rR \left[\rho \left(\frac{\eta R}{nB_o} \frac{q^{(o)}}{dq^{(o)}/dr} \right)^2 \right]^{1/6} \quad . \tag{A27}$$

(This variable X should not be confused with the coordinate entering Eq. (4) which measure the distance from the axis of symmetry.)

To determine the analogous macroscopic variable Y , defined by

$$Y \equiv (V-V_o)/V_S \quad , \tag{A28}$$

where V_S is an unspecified macroscopic scale factor, we choose

$$V_S = dV/dr = 4\pi^2 rR \quad , \tag{A29}$$

so that

$$Y = r-r_o \tag{A30}$$

in accordance with the literature on cylindrical model tokamaks. Then the large ratio which enters the dispersion relation in Ref. 6 is given by

$$\frac{V_S}{X_o} = \left[\frac{1}{\rho}\left(\frac{nB_o}{\eta R}\,\frac{dq^{(o)}/dr}{q^{(o)}}\right)^2\right]^{1/6} . \tag{A31}$$

The characteristic length within the singular layer is given by

$$\delta r = \left[\rho\left(\frac{\eta R}{nB_o}\,\frac{q^{(o)}}{dq^{(o)}/dr}\right)^2\right]^{1/6} |Q|^{1/4} . \tag{A32}$$

This can be regarded as the thickness of the singular layer.

REFERENCES

* On loan from Westinghouse Research Laboratories.

[1]S. V. Mirnov and I. V. Semenov, in Plasma Physics and Controlled Nuclear Fusion Research (International Atomic Energy Agency, VIENNA, 1971), Vol. II, P. 401; Zh. Eksp. Teor. Fiz. 60, 2105 (1971) [Phys.-JETP 33, 1134 (1971)].

[2]J. C. Hosea, C. Bobeldijk, and D. J. Grove, in Plasma Physics and Controlled Nuclear Fusion Research (International Atomic Energy Agency, VIENNA, 1971), Vol. II, p. 425.

[3]H. P. Furth, J. Killeen, and M. N. Rosenbluth, Phys. Fluids 6, 459 (1963).

[4]B. Coppi, J. M. Greene, and J. L. Johnson, Nucl. Fusion 6, 101 (1966).

[5]H. P. Furth, P. H. Rutherford, and H. Selberg, Phys. Fluids 16, 1054 (1973).

[6]A. H. Glasser, J. M. Greene, and J. L. Johnson, Phys. Fluids 18, 875 (1975).

[7]J. D. Jackson, Classical Electrodynamics (Wiley, New York 1962), p. 618.

[8]S. Yoshikawa, Phys. Fluids 17, 178 (1974).

[9]An equivalent expression was obtained by A. B. Mikhailovskii, Nucl. Fusion 15, 95 (1975).

[10]H. P. Furth, M. N. Rosenbluth, P. H. Rutherford, and W. Stodiek, Phys. Fluids 13, 3020 (1970).

[11]L. Spitzer and R. Härm, Phys. Rev. 89, 5 (1953).

[12]B. Coppi, Phys. Fluids 7, 1501 (1964).

[13]E. Frieman, K. Weimer, and P. Rutherford, Plasma Physics and Controlled Nuclear Fusion Research (International Atomic Energy Agency, VIENNA, 1966) Vol. 1, p. 595.

[14]P. H. Rutherford and H. P. Furth, Princeton University MATT 872 (1971).

[15]R. D. Hazeltine, D. Dobrott, and T. S. Wang, Phys. Fluids, to be published.

[16]P. H. Rutherford and E. A. Frieman, Phys. Fluids 11, 569 (1968).

[17]The factor (1-H/2) in the denominator of Eq. (111) of Ref. (6) should be $\Gamma(1-H/2)$, as in Eq. (87) of that work.

[18]M. S. Chance, R. L. Dewar, A. H. Glasser, J. M. Greene, R. C. Grimm, S. C. Jardin, J. L. Johnson, B. Rosen, G. V. Sheffield, and K. E. Weimer, in Plasma Physics and Controlled Nuclear Fusion Research (International Atomic Energy Agency, VIENNA, 1974), Paper IAEA-CN-33/A12-4.

[19]M. N. Rosenbluth, R. Y. Dagazian, and P. H. Rutherford, Phys. Fluids 16, 1894 (1973).

[20]G. Laval, Phys. Rev. Letters 34, 1316 (1975).

[21]R. Pellat, private communication.

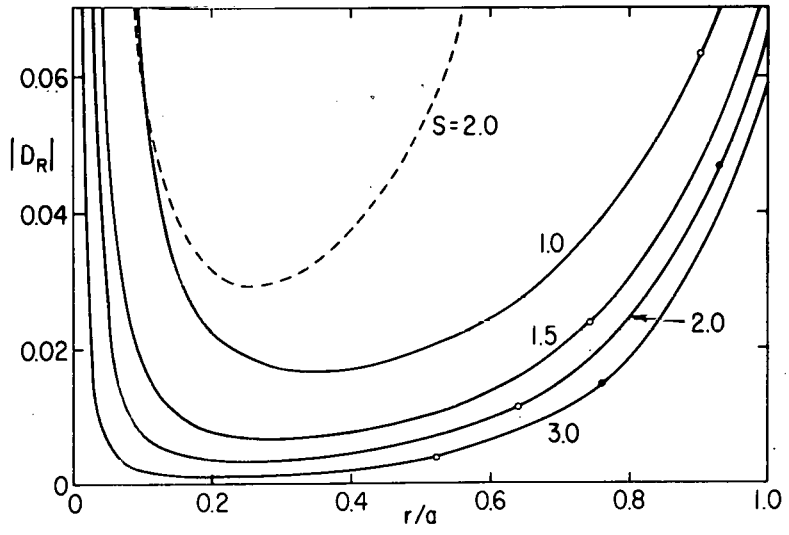

752237

Fig. 1. The parameter $|D_R|$, Eq. (22), as a function of the minor radius in the ST and PLT tokamaks. The solid curves are for ST for several values of the shear parameter s. The dashed curve is for PLT with s = 2.0. Open circles indicate the q = 2 surface, solid circles the q = 3 surfaces.

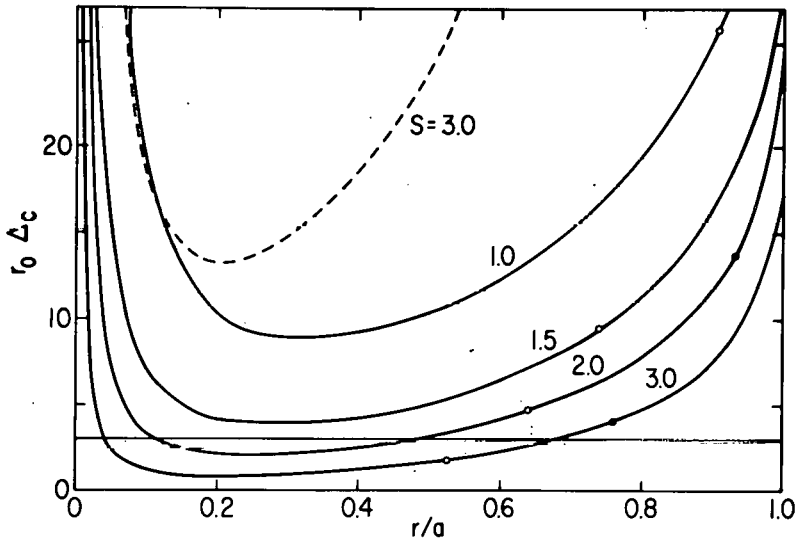

752261

Fig. 2. The dimensionless parameter $r_o\Delta_C$ as a function of minor radius, with Δ_C given by Eq. (15) and r_o the shear scale length $a/\sqrt{s}$. The solid curves are for ST; the dashed curve is for PLT. The horizontal line denotes the value of $r_o\Delta$ calculated in Ref. 5 for the m = 2 mode. This mode goes unstable when the open circle denoting the q = 2 surface falls below the line. The larger values of $r_o\Delta_C$ for PLT indicate greater stability.

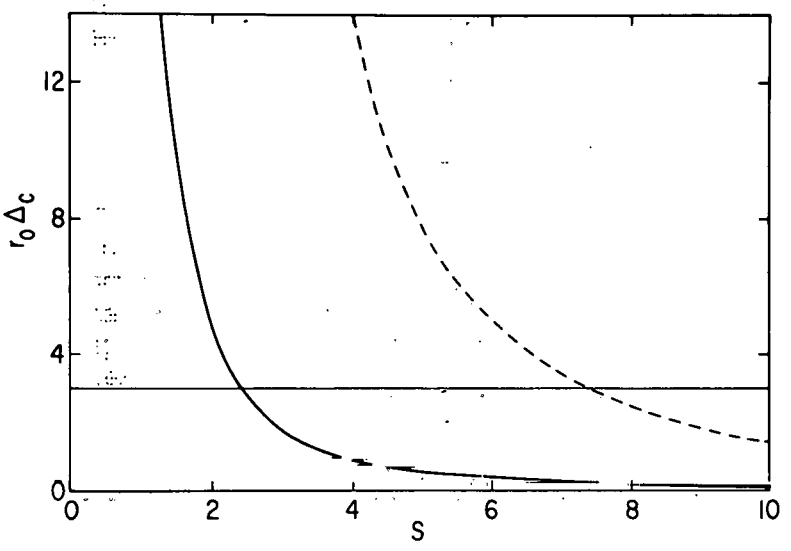

Fig. 3. The quantity $r_o\Delta_c$ at the q = 2 surface as a function of the shear parameter s. The solid curve shows that the m = 2 mode in ST goes unstable when s reaches 2.4 and $r_o\Delta_c$ falls below the horizontal line representing $r_o\Delta$. The dashed curve shows that this mode remains stable in PLT until s reaches 7.5.

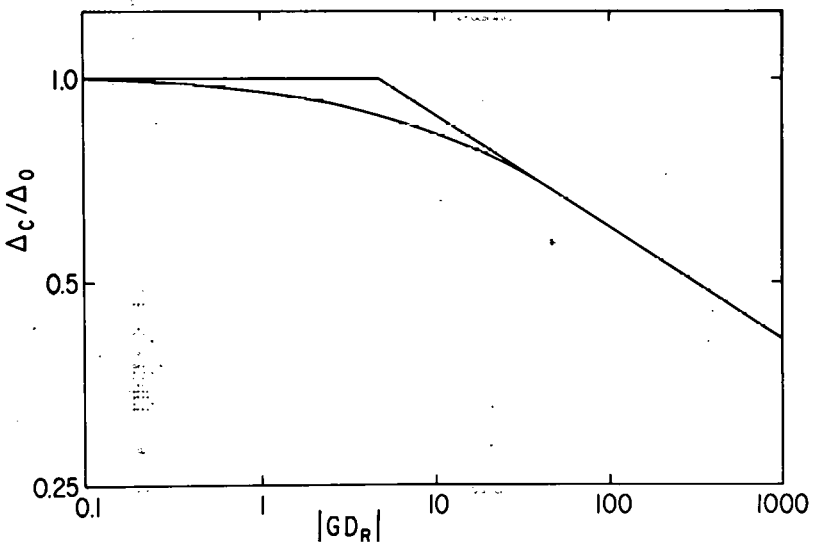

Fig. 4. Log-log plot of the ratio Δ_c/Δ_o as a function of $|GD_R|$, with Δ_c obtained numerically from Eq. (A9) of Ref. 6 and Δ_o the value of Δ_c when Q = 0, given by Eq. (15). Straight lines show the asymptotic behavior given by Eqs. (15) and (23).

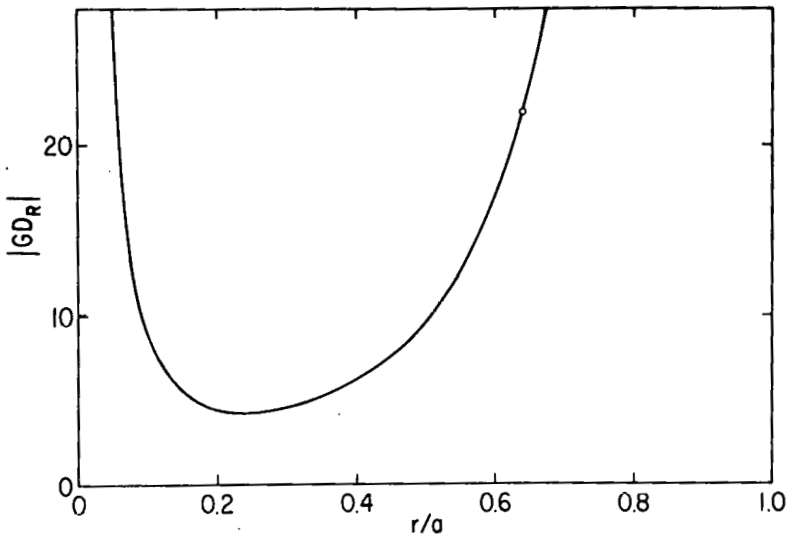

752242

Fig. 5. $|GD_R|$ as a function of the minor radius in ST and PLT with s = 2.0. The circle denotes the q = 2 surface.

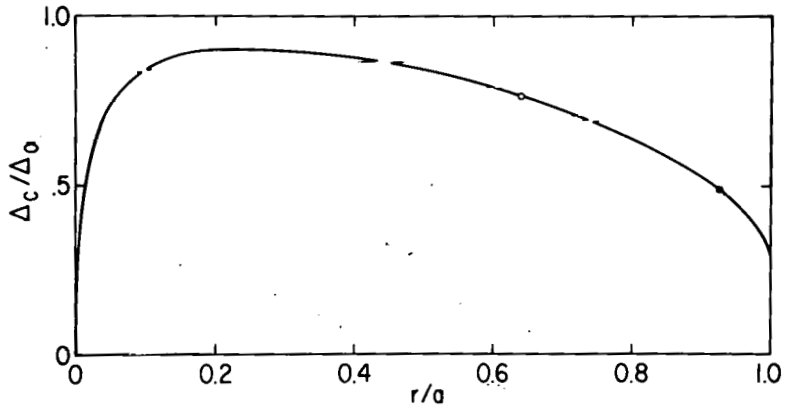

752243

Fig. 6. Δ_c/Δ_o as a function of the minor radius in ST and PLT with s = 2, in response to the variation of $|GD_R|$ as shown in Figs. 4 and 5.

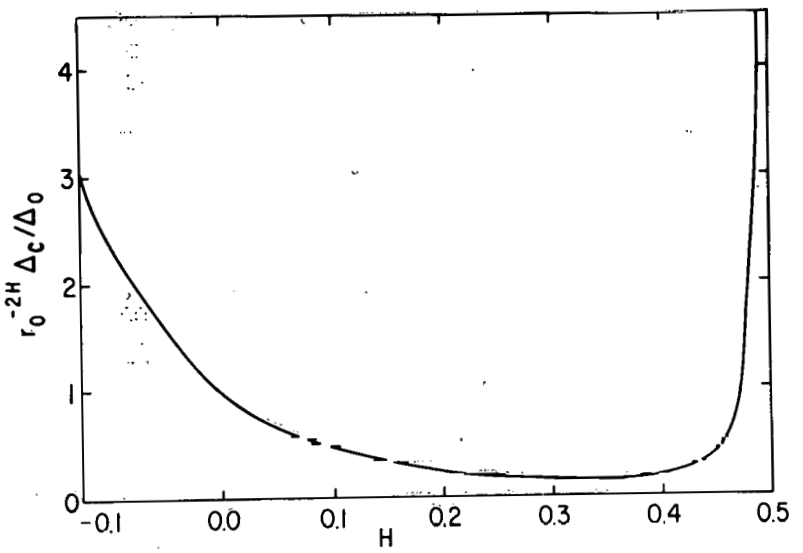

752238

Fig. 7. The dimensionless ratio $r_o^{-2H}\Delta_c/\Delta_o$ as a function of H, with Δ_c given by Eq. (111) of Ref. 6, Δ_o given by Eq. (15), $D_R = -0.01$, and $r_o\nabla_s/X_o = 250$.

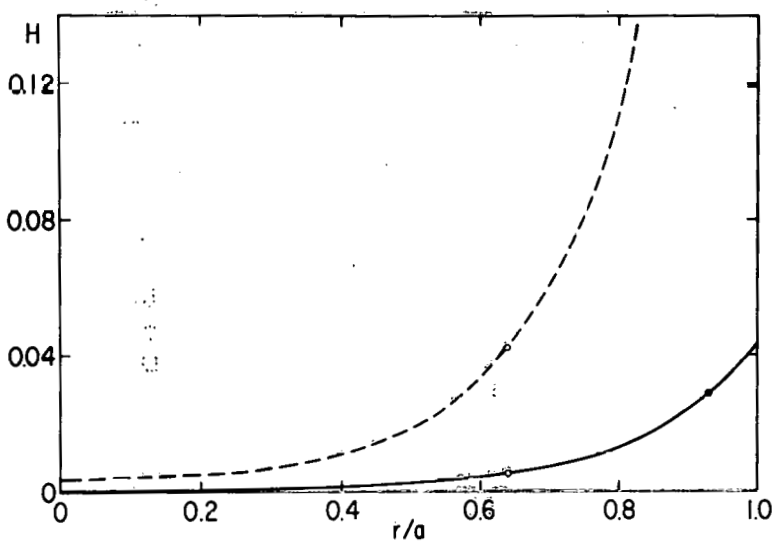

752239

Fig. 8. The parameter H, Eq. (27), as a function of the minor radius. The solid curve is for ST, the dashed curve for PLT, both for s = 2.0. Open circles denote q = 2 surfaces, solid circles q = 3 surfaces.

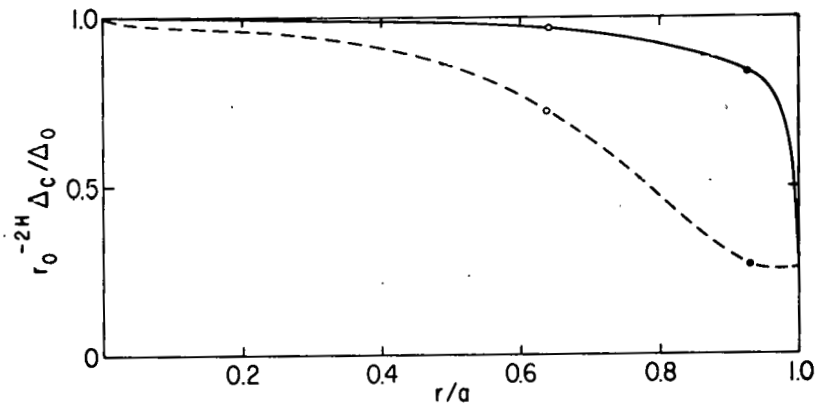

752236

Fig. 9. The ratio $r_0^{-2H}\Delta_c/\Delta_0$ as a function of the minor radius, in response to the variation of H as shown in Figs. 7 and 8.